Evolution Equations for Continuous-Scale Morphological Filtering

Roger W. Brockett, *Fellow, IEEE*, and Petros Maragos, *Senior Member, IEEE*

Abstract—**Multiscale signal analysis has recently emerged as a useful framework for many computer vision and signal processing tasks. Morphological filters can be used to develop nonlinear multiscale operations that have certain advantages over linear multiscale approaches in that they preserve important signal features such as edges. In this paper, we discuss several nonlinear partial differential equations that model the scale evolution associated with continuous-space multiscale morphological erosions, dilations, openings, and closings. These equations relate the rate of change of the multiscale signal ensemble as scale increases to a nonlinear operator acting on the space of signals. The nonlinear operator is characterized by the shape and dimensionality of the structuring element used by the morphological operators, generally taking the form of a nonlinear function of certain partial differential operators.**

I. Introduction

BOTH in computer vision and video data compression, important problems such as feature detection, motion detection, and multiband frequency analysis often require analyzing the image signals at multiple spatial scales or resolutions. Motivations include the already successful scenarios of

i) detecting events (e.g., edges, peaks, motion displacements) at large scales and then refining their location or value at smaller scales [19], [31], [6], [22]
ii) subband image coding [32]
iii) solving estimation problems for multiresolution stochastic processes [30].

Recently, such problems have been addressed using *multiscale signal analysis*. In most of the work in this area, the multiscale versions of an image have been obtained by acting on the image with a *linear* smoothing filter whose impulse response is a Gaussian with variance proportional to scale. There is, however, a variety of *nonlinear* smoothing filters, including the morphological openings and closings [20], [24], [15] and the anisotropic and nonlinear diffusion schemes in [21] and [13], that can provide a multiscale image ensemble and have the advantage over the linear Gaussian smoothers in that they do not blur or shift image edges. This attractive property of morphological smoothers is illustrated in Fig. 1.

In this paper, we study multiscale morphological operators. Multiscale openings and closings (also known as 'granulometries') of binary images were first developed by Matheron [20] in his theory of size distributions. They have been used extensively in image analysis applications of mathematical morphology to biology and petrography [24]. They have also been applied as general nonlinear smoothers for multiscale shape description and representation via shape-size histograms and skeleton transforms [15], [17]. Scale-space zero-crossing maps of multiscale openings of 1-D boundary curvature functions were shown in [7] to possess a causality property similar to that of Gaussian scale-space maps in [31], [1], and [33]. In addition, openings and closings were used for signal smoothing and reconstruction in multiresolution morphology [9]. Further, multiscale openings and closings can be used to generate a class of efficient nonlinear smoothing filters, called 'alternating sequential filters,' which smooth progressively from the smallest scale possible up to a maximum scale by using alternating compositions of openings and closings [27], [16], [25], [23], [26]. The use of morphological operators for multiscale signal analysis is not limited to operations of a smoothing type. For instance, in fractal image analysis, nonlinear operators such as the morphological erosion and dilation can provide multiscale distributions of the shrink-expand type from which the fractal dimension can be computed [18].

Thus far, most of the multiscale image filtering implementations have been discrete. However, due to the current interest in analog VLSI and neural networks, there is renewed interest in analog computation, e.g., see [3]. For computer vision tasks, Witkin [31] proposed a continuous (in scale s and signal argument x) multiscale signal ensemble

$$\gamma(x, s) = f(x) * G_s(x) \tag{1}$$

where an original signal f is convolved with a Gaussian function

$$G_s(x) = \frac{1}{\sqrt{4\pi s}} \exp\left(-\frac{x^2}{4s}\right) = \frac{1}{\sigma\sqrt{2\pi}} \exp\left(-\frac{x^2}{2\sigma^2}\right) \tag{2}$$

whose standard deviation $\sigma = \sqrt{2s}$ is proportional to the square root of the scale parameter s. This Gaussian scale space has been studied extensively in the computer vision literature, e.g., see [11], [1], [33], [10]. It is well known (e.g., in [11]) that the Gaussian multiscale function γ can be generated from

Manuscript received June 12, 1993; revised April 11, 1994. This work was supported by the ARO under Grant DAALO3-86-K-0171 to the Center for Intelligent Control Systems, by the NSF under Grant MIP-8658150 with matching funds from Xerox, and by NSF under Grant MIP-9396301. The associate editor coordinating the review of this paper and approving it for publication was Dr. Thomas F. Quatieri, Jr.

R. Brockett is with the Division of Applied Sciences, Harvard University, Cambridge, MA 02138 USA.

P. Maragos is with the School of Electrical and Computer Engineering, Georgia Institute of Technology, Atlanta, GA 30332 USA.

IEEE Log Number 9406025.

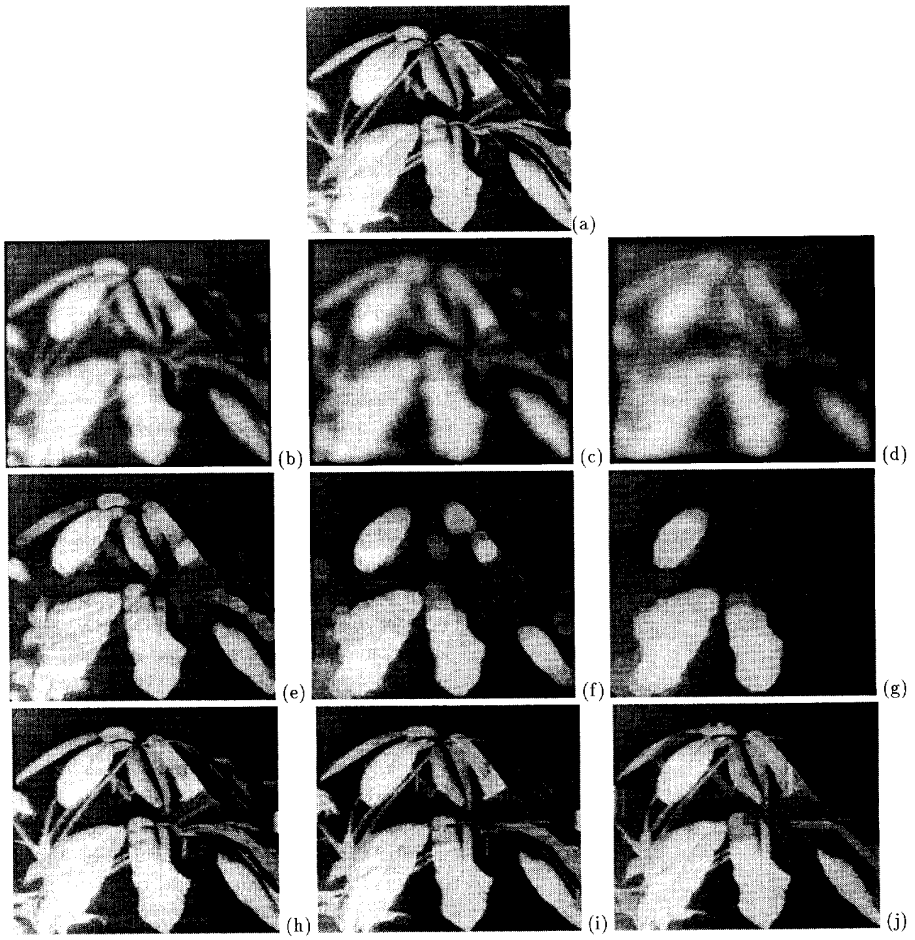

Fig. 1. (a) Original image f (220 × 256 pixels). Linear smoothings (*b*, *c*, *d*) via convolution of f with a Gaussian of standard deviation; (b) $\sigma = 2.25$; (c) $\sigma = 4.25$; (d) $\sigma = 6.25$. Morphological smoothings (*e*, *f*, *g*) via opening of f by an octagon of (e) size = 2; (f) size = 4; (g) size = 6. (The unit-size octagon is a discrete disk of radius $\sqrt{5}$; the n-size octagon is an n-fold dilation of the unit octagon with itself and has a width of $4n + 1$ pixels.) Morphological smoothings (h, i, j) via radial opening of f, i.e., by taking the maximum of four openings of f by four linear segments oriented at 0, 45, 90, and 135° and each of size (in number of pixels) equal to (h) size = 9; (i) size = 17; (j) size = 25.

the diffusion equation

$$\frac{\partial \gamma}{\partial s} = \frac{\partial^2 \gamma}{\partial x^2} \tag{3}$$

starting from the initial condition $\gamma(x, 0) = f(x)$. This partial differential equation (PDE) represents a continuous dynamical system that generates this multiscale convolution of f. In [21] and [13], there are nonlinear versions of this idea.

This paper is an enlarged version of our work in [4]. Our main contribution is to develop nonlinear PDE's modeling multiscale morphological operators of the shrink-expand type (erosions/dilations) and of the smoothing type (openings/closings). Given a signal $f(x)$, we generally define its multiscale morphological transformation as a space-scale function $\psi(x, s)$, which at each scale s represents the transformation of $f(x)$ by a structuring element of size $s \geq 0$. The nonlinear PDE's we developed can be viewed as *dynamical systems* that, starting from the initial condition $\psi(x, 0) = f(x)$, generate the multiscale function $\psi(x, s)$ as output. They can also be viewed as describing the *scale evolution* of these multiscale operators, meaning that they provide the rule by which the rate of change of $\psi(x, s)$ in scale direction s is related to the rates of change in spatial directions x. Our motivations in this work have been the wide applicability of multiscale morphological filtering as well as the potential applications of continuous dynamical systems. In addition, the theory of morphological operators had thus far been based on set and lattice theory. A novel by-product of our work is now the ability to use calculus-based tools to analyze them, which might make easier to connect them with physical applications.

The basic ingredients of multiscale morphology are multiscale erosions and dilations. For example, morphological openings and closings are compositions of erosions and dilations. Hence, the biggest part of our analysis (Section II) focuses on deriving the nonlinear PDEs modeling the scale evolution of a variety of multiscale erosions and dilations. These PDE's are nonlinear functions of first-order partial

differential operators, and their form varies according to the shape and dimensionality of the structuring element. This part of our work can be viewed as describing a nonlinear scale-space based on min-max operators rather than being an extension of multiscale Gaussian convolutions. As multiscale dilations and erosions propagate, they can create a kind of shock-wave phenomenon; thus, it is not too surprising that they are related to Burger's 1-D equation [5], [12]. In [29], the solution to Burger's equation is interpreted as a multiscale dilation. The work in ch. 8 of [29] is related to ours, as will be discussed later. In Section III, we present a PDE for multiscale opening and closing, which involves both differential and difference operators. Finally, we conclude in Section IV with some brief discussion on

i) infinitesimal generators of multiscale operators
ii) modeling multiscale analog rank-order filters (e.g., analog medians [8], [14]), which are closely related to morphological filters
iii) how to extend the work in this paper to a hybrid linear and nonlinear multiscale scheme.

II. Multiscale Dilations and Erosions

Henceforth, let $f : \mathbf{R}^d \to \mathbf{R}$ be a function representing some d-dimensional signal $d = 1, 2, 3, \ldots$, and let the '*structuring function*' $g : B \to \mathbf{R}$ represent some structuring element with compact support $B \subseteq \mathbf{R}^d$. The morphological dilation $f \oplus g$ and erosion $f \ominus g$ of f by g are defined [24], [27], [17] by

$$(f \oplus g)(x) \triangleq \sup\{f(x - v) + g(v) : v \in B\}, \quad x \in \mathbf{R}^d$$
$$(f \ominus g)(x) \triangleq \inf\{f(x + v) - g(v) : v \in B\}, \quad x \in \mathbf{R}^d.$$

To define *multiscale* dilations and erosions, we consider dilating and eroding f by a multiscale version $g_s : sB \to \mathbf{R}$ of the structuring function g, where

$$sB \triangleq \{sb : b \in B\}, \quad s \geq 0 \tag{4}$$
$$g_s(x) \triangleq sg(x/s), \quad s > 0 \tag{5}$$

and s is the continuous *scale parameter*. If $s = 0$, then $sB = \{\vec{0}\}$, and $g_0(\vec{0}) = 0$. The function g_s has the same shape as g, but both its domain and range are scaled by a factor s. Specifically, let

$$U(g) \triangleq \{(x, a) \in \mathbf{R}^d \times \mathbf{R} : a \leq g(x)\} \tag{6}$$

be the 'umbra' of g (this is also called 'hypograph' in convex analysis). Then

$$U(g_s) = sU(g) \tag{7}$$

and thus, the support of g_s is the set B scaled by s. The multiscale dilation and erosion of f by g at scale s are defined as the functions

$$\delta(x, s) \triangleq (f \oplus g_s)(x) = \sup_{v \in sB}\{f(x - v) + sg(v/s)\} \tag{8}$$
$$\varepsilon(x, s) \triangleq (f \ominus g_s)(x) = \inf_{v \in sB}\{f(x + v) - sg(v/s)\}. \tag{9}$$

Note that

$$\delta(x, 0) = \varepsilon(x, 0) = f(x). \tag{10}$$

Further, if f and g are continuous, the multiscale functions δ and ε remain continuous at all x and s.

If $g : B \to \{0\}$ is constant and equal to zero, it is usually called a *flat* structuring function, and the dilation and erosion by g_s become the following moving sup and inf of the input signal inside the moving window set sB:

$$(f \oplus sB)(x) \triangleq \sup\{f(x - v) : v \in sB\} \tag{11}$$
$$(f \ominus sB)(x) \triangleq \inf\{f(x + v) : v \in sB\}. \tag{12}$$

We refer to the above operations as *multiscale dilations/erosions by a structuring set* (B) because the function g carries the same information with its support set B. Morphological operators that use structuring sets are simpler to analyze and implement than their counterparts that use nonflat structuring functions, and they have found more applications. Hence, we dedicate a significant part of this paper to their analysis.

Our primary goal in this paper is to attempt to make sense out of the following evolution:

$$\frac{\partial \delta}{\partial s}(x, s) = \lim_{r \downarrow 0} \frac{\delta(x, s + r) - \delta(x, s)}{r} \tag{13}$$

for δ and to interpret its solution in morphological terms. Toward this goal, we henceforth constrain g to be *nonnegative* and *concave* (i.e., have a convex umbra); hence, B is convex as well. Since B is compact and convex, it is well known from [20] and [24] that the set collection $\{sB : s \geq 0\}$ forms a one-parameter semigroup with respect to the set dilation operation. Specifically

$$sB \oplus rB = (s + r)B \tag{14}$$

where the set dilation $\oplus$ is defined as the Minkowski set addition

$$X \oplus Y \triangleq \{x + y : x \in X, y \in Y\}, \quad X, Y \subseteq \mathbf{R}^d. \tag{15}$$

Further, dilations and erosions satisfy the following laws [24]:

$$(f \oplus g) \oplus h = f \oplus (g \oplus h) \tag{16}$$
$$(f \ominus g) \ominus h = f \ominus (g \oplus h). \tag{17}$$

Hence, if $\mathcal{D}_s(f) = f \oplus sB$ and $\mathcal{E}_s(f) = f \ominus sB$ denote the multiscale operators, we have

$$\mathcal{D}_s(\mathcal{D}_r(f)) = \mathcal{D}_{s+r}(f) \tag{18}$$
$$\mathcal{E}_s(\mathcal{E}_r(f)) = \mathcal{E}_{s+r}(f). \tag{19}$$

Thus, the multiscale dilation and erosion by a compact convex structuring set have a *semigroup* structure. For multiscale dilations/erosions by functions, note that $U(g_s) \oplus U(g_r) = U(g_{s+r})$ because of the convexity of $U(g)$; hence, $g_s \oplus g_r = g_{s+r}$. Therefore, the corresponding multiscale operators defined by $\mathcal{D}_s(f) = f \oplus g_s$ and $\mathcal{E}_s(f) = f \ominus g_s$ also satisfy (18) and (19) and thus have a semigroup structure. A more general discussion of semigroup structures of morphological operators can be found in [25].

From the semigroup structure of multiscale dilations/erosions, it follows that

$$\delta(x, s+r) = \delta(x, s) \oplus g_r(x) \tag{20}$$

$$\varepsilon(x, s+r) = \varepsilon(x, s) \ominus g_r(x). \tag{21}$$

Therefore, the evolution (13) for the multiscale dilation and its corresponding law for the multiscale erosion become

$$\frac{\partial \delta}{\partial s}(x, s) = \lim_{r \downarrow 0} \frac{\sup_{v \in rB}\{\delta(x-v, s) + rg(v/r)\} - \delta(x, s)}{r} \tag{22}$$

$$\frac{\partial \varepsilon}{\partial s}(x, s) = \lim_{r \downarrow 0} \frac{\inf_{v \in rB}\{\varepsilon(x+v, s) - rg(v/r)\} - \varepsilon(x, s)}{r}. \tag{23}$$

Next, we discuss multiscale versions of dilations and erosions by 1-D and 2-D sets and functions and develop PDE's that model their multiscale evolution. These results will involve relating the right sides of (22) and (23) to nonlinear functions of $\partial\delta/\partial x$ and $\partial\varepsilon/\partial x$.

A. Dilations/Erosions by 1-D Sets

Given a differentiable function $f : \mathbf{R} \to \mathbf{R}$, let $B = [-1, 1]$ assume a flat $g : B \to \{0\}$, and let

$$\delta(x, s) = (f \oplus sB)(x), \quad \varepsilon(x, s) = (f \ominus sB)(x).$$

Fig. 2 shows examples of such scale-space functions ε and δ. The following result is the observation that δ and ε satisfy a rather simple but nonlinear partial differential equation at points where the data are smooth.

Theorem 1: If the partial derivatives $\partial\delta/\partial x$ and $\partial\varepsilon/\partial x$ exist at some point x and scale s, then

$$\frac{\partial \delta}{\partial s}(x, s) = \left|\frac{\partial \delta}{\partial x}(x, s)\right| \tag{24}$$

$$\frac{\partial \varepsilon}{\partial s}(x, s) = -\left|\frac{\partial \varepsilon}{\partial x}(x, s)\right|. \tag{25}$$

Proof: Using a first-order Taylor's formula and denoting $\delta_x = \partial\delta/\partial x$, we have

$$\delta(x+v, s) - \delta(x, s) = \delta_x v + |v| o(v)$$

where $o(v) \to 0$ as $v \to 0$. Thus, since we will consider v in $[-r, r]$, by ignoring the term with $o(v)$ in the limit $r \downarrow 0$, we can write (22) as

$$\frac{\partial \delta}{\partial s}(x, s) = \lim_{r \downarrow 0} \frac{\sup\{\delta_x v : |v| \le r\}}{r} = \lim_{r \downarrow 0} \frac{|\delta_x| r}{r} = \left|\frac{\partial \delta}{\partial x}\right|$$

which proves (24). The proof is similar for ε by replacing sup with inf. □

Thus, assuming that the partial derivatives $\partial\delta/\partial x$ and $\partial\varepsilon/\partial x$ are continuous, these two nonlinear PDE's can generate the 1-D multiscale dilations and erosions starting from the initial conditions $\delta(x, 0) = \varepsilon(x, 0) = f(x)$. However, even if f is differentiable, as the scale s increases, the multiscale erosions/dilations can create discontinuities in their derivatives $\partial/\partial x$; then these derivatives and the generator PDE's have to be interpreted correctly at such points according to the specific

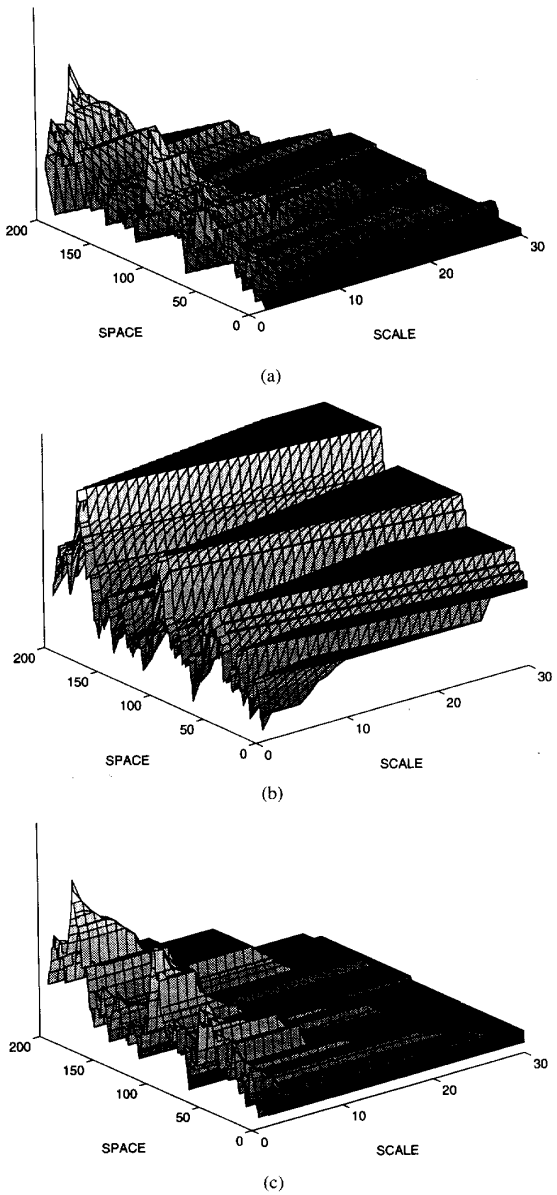

Fig. 2. Multiscale (a) erosion, (b) dilation, and (c) opening of a 1-D signal $f(x)$, which is the last 200-sample part of the original signal in Fig. 3 by a structuring set $B = \{-1, 0, 1\}$ for scales $s = 0, 1, \ldots, 30$.

case. To solve this problem, we can replace the conventional derivatives with 'morphological derivatives.' Specifically, we define the morphological *sup-derivative*[1] M of a 1-D real continuous function f at a point x as follows:

$$M(f)(x) \triangleq \lim_{r \downarrow 0} \frac{\sup\{f(x+v) : |v| \le r\} - f(x)}{r}. \tag{26}$$

Note that the average dilation-erosion symmetric derivative $[M(f) + M(-f)]/2$ is equal to Beucher's morphological gradient [2], [24]. By using a similar type of proof as in

[1] Note that the dual inf-derivative $\lim_{r \downarrow 0}[f(x) - \inf\{f(x+v) : |v| \le r\}]/r$ is equal to $M(-f)(x)$.

Theorem 1, the following relationships can be proven between the morphological and standard derivatives: Let $f : \mathbf{R} \to \mathbf{R}$ be continuous, and let its right derivative $f'(x+) = \lim_{r \downarrow 0}[f(x+r) - f(x)]/r$ and its left derivative $f'(x-)$ exist at some point x. Then, it can be shown that

$$M(f)(x) = \max[0, f'(x+), -f'(x-)] \tag{27}$$

$$f'(x+) = f'(x-) = f'(x) \Longrightarrow M(f)(x) = |f'(x)|. \tag{28}$$

Thus, if $df(x)/dx$ exists, then $M(f)(x)$ is equal to the magnitude of the standard derivative. If, however, df/dx does not exist at x, then the M derivative still gives a valid answer related to the magnitudes of the left and right derivatives at x.

Hence, a more general form of the dilation PDE results from replacing the $|\partial\delta/\partial x|$ in (24) with $M_x(\delta)$, where M_x is the partial sup-derivative in the x direction, i.e.

$$M_x(\delta)(x,s) \triangleq \lim_{r \downarrow 0} \frac{\sup\{\delta(x+v,s) : |v| \le r\} - \delta(x,s)}{r}. \tag{29}$$

Similarly, a more general form of the erosion PDE results from replacing the $|\partial\varepsilon/\partial x|$ in (25) with $M_x(-\varepsilon)$. Thus, the PDEs in (24) and (25) are special cases (when $\partial\delta/\partial x$ and $\partial\varepsilon/\partial x$ are continuous) of the following more general PDE's:

$$\frac{\partial\delta}{\partial s} = M_x(\delta) \tag{30}$$

$$\frac{\partial\varepsilon}{\partial s} = -M_x(-\varepsilon). \tag{31}$$

These general forms allow the dilation and erosion PDE's to still hold even if discontinuities are created in the partial derivatives $\partial\delta/\partial x$ and $\partial\varepsilon/\partial x$ as the scale increases, provided that the equations evolve in such a way as to give solutions that are piecewise differentiable with left and right limits at each point.

B. Dilations/Erosions by 2-D Sets

Given a differentiable function $f : \mathbf{R}^2 \to \mathbf{R}$, we can find similar PDE's (as in Section II-A) for its multiscale dilations and erosions

$$\delta(x,y,s) = (f \oplus sB)(x,y)$$

$$\varepsilon(x,y,s) = (f \ominus sB)(x,y)$$

by a 2-D convex compact structuring set B. The only difference now is that the shape of B affects the form of the PDE. The following theorem summarizes the results for three different shapes of B, i.e., a unit *diamond*, a unit *disk*, and a unit *square*.

Theorem 2: If the partial derivatives along the x and y directions of δ and ε exist and are continuous at some point (x,y) and scale s, then:

If $B = \{(v,u) : |v| + |u| \le 1\}$ (diamond)

$$\frac{\partial\delta}{\partial s}(x,y,s) = \max\left\{\left|\frac{\partial\delta}{\partial x}\right|, \left|\frac{\partial\delta}{\partial y}\right|\right\}. \tag{32}$$

If $B = \{(v,u) : v^2 + u^2 \le 1\}$ (disk)

$$\frac{\partial\delta}{\partial s}(x,y,s) = \sqrt{\left|\frac{\partial\delta}{\partial x}\right|^2 + \left|\frac{\partial\delta}{\partial y}\right|^2}. \tag{33}$$

If $B = \{(v,u) : |v|, |u| \le 1\}$ (square)

$$\frac{\partial\delta}{\partial s}(x,y,s) = \left|\frac{\partial\delta}{\partial x}\right| + \left|\frac{\partial\delta}{\partial y}\right|. \tag{34}$$

The multiscale erosions ε satisfy equations identical to these above except that one must multiply the right-hand sides by -1.

Proof: Using a first-order Taylor's formula and denoting $\delta_y = \partial\delta/\partial y$, we have

$$\delta(x+v,y+u,s) - \delta(x,y,s) = \delta_x v + \delta_y u + \|(v,u)\| o(\|(v,u)\|)$$

where $o(\|(u,v)\|) \to 0$ as $\|(v,u)\| \to 0$. Thus, by ignoring in the limit the term with $o()$, we can write (22) as

$$\frac{\partial\delta}{\partial s} = \lim_{r \downarrow 0} \frac{\sup\{\delta_x v + \delta_y u : (v,u) \in rB\}}{r}.$$

Because the function $\delta_x v + \delta_y u$ is linear in u and v, over the compact domain rB, it assumes its maximum value on the boundary of rB. In addition, in view of the symmetry of rB with respect to the x, y axes, we have

$$\sup_{(v,u) \in rB} \{\delta_x v + \delta_y u\} = \max_{0 \le v \le r} \{|\delta_x| v + |\delta_y| b(v)\}$$

where the boundary function $b : [0,r] \to [0,r]$ is defined by

$$b(v) = \begin{cases} r - v, & \text{if } B = \text{diamond} \\ \sqrt{r^2 - v^2}, & \text{if } B = \text{disk} \\ r, & \text{if } B = \text{square} \end{cases}$$

Hence

$$\sup_{(v,u) \in rB} \{\delta_x v + \delta_y u\} = \begin{cases} r \cdot \max(|\delta_x|, |\delta_y|), & B = \text{diamond} \\ r\sqrt{\delta_x^2 + \delta_y^2}, & B = \text{disk} \\ r(|\delta_x| + |\delta_y|), & B = \text{square} \end{cases}$$

from which (32)–(34) directly follow. Similar analysis applies to ε, replacing sup with inf; we omit the details. □

Thus, if $\partial\delta/\partial x, \partial\delta/\partial y$ and $\partial\varepsilon/\partial x, \partial\varepsilon/\partial y$ remain continuous for all scales s, we can use the previous PDE's to generate the multiscale ensembles δ and ε, starting from the initial condition

$$\delta(x,y,0) = \varepsilon(x,y,0) = f(x,y)$$

Otherwise, if the one-sided x, y partial derivatives of δ and ε exist everywhere, then we can use generalized forms of these PDE's where the standard derivatives are replaced by morphological sup-and inf-derivatives, as in the 1-D case described by (29)–(31).

C. Dilations/Erosions by Functions

Let $f : \mathbf{R} \to \mathbf{R}$ be a differentiable function, and let $g : [-1,1] \to \mathbf{R}$ be a continuous nonnegative and concave structuring function. Then, it is possible to find PDE's for the multiscale dilations and erosions

$$\delta(x,s) = (f \oplus g_s)(x), \quad \varepsilon(x,s) = (f \ominus g_s)(x)$$

which are more general than those in Section II-A. We present results for three different shapes of g, where the graph of g

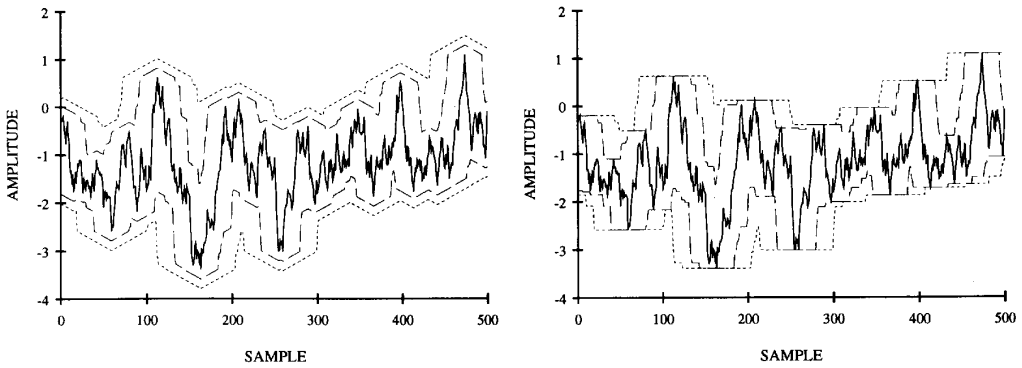

(a) (b)

Fig. 3. One-dimensional sampled signal (solid line) and its erosions (two lower dashed lines) and dilations (two upper dashed lines) by g_s at scales s =20, 40, where g is a three-sample sequence: (a) Triangular $g : g(0) = 0.01$, $g(-1) = g(1) = 0$; (b) flat rectangular $g : g(-1) = g(0) = g(1) = 0$ (from [18]).

is the top boundary of one of the three planar sets used in Section II-B scaled by $g(0) \geq 0$, that is, g is defined as

$$g(x) = g(0) \sup\{y : (x, y) \in B\} \tag{35}$$

where B is the unit diamond, disk, or square.

Theorem 3: If δ and ε are the multiscale dilations and erosions appearing above, and if $\partial\delta/\partial x$ and $\partial\varepsilon/\partial x$ exist at some point x and scale s, then:

If $g(x) = g(0)(1 - |x|)$, $|x| \leq 1$, (triangular)

$$\frac{\partial \delta}{\partial s}(x, s) = \max\left\{\left|\frac{\partial \delta}{\partial x}\right|, g(0)\right\}. \tag{36}$$

If $g(x) = g(0)\sqrt{1 - x^2}$, $|x| \leq 1$, (circular)

$$\frac{\partial \delta}{\partial s}(x, s) = \sqrt{\left|\frac{\partial \delta}{\partial x}\right|^2 + g^2(0)}. \tag{37}$$

If $g(x) = g(0)$, $|x| \leq 1$, (rectangular)

$$\frac{\partial \delta}{\partial s}(x, s) = \left|\frac{\partial \delta}{\partial x}\right| + g(0). \tag{38}$$

The multiscale erosions ε satisfy equations identical to these above except that one must multiply the right-hand sides by -1.

Proof: From (22), it follows that

$$\frac{\partial \delta}{\partial s} = \lim_{r \downarrow 0} \frac{\sup\{\delta_x v + r g(v/r) : |v| \leq r\}}{r}.$$

Since g is even and nonnegative over $[-1, 1]$, we have

$$\begin{aligned} &\sup_{|v| \leq r} \{\delta_x v + r g(v/r)\} \\ &\quad = \max_{0 \leq v \leq r} \{|\delta_x| v + r g(v/r)\} \\ &\quad = \begin{cases} r \cdot \max(|\delta_x|, g(0)), & g = \text{triangular} \\ r\sqrt{|\delta_x|^2 + g^2(0)}, & g = \text{circular} \\ r(|\delta_x| + g(0)), & g = \text{rectangular} \end{cases} \end{aligned}$$

from which (36)–(38) directly follow. This is similar for ε by replacing sup with inf.

Thus, if $\partial\delta/\partial x$ and $\partial\varepsilon/\partial x$ remain continuous at all (x, s), the above PDE's model the scale evolution of the general dilations and erosions. Discontinuities in the derivative $\partial/\partial x$ can be handled by using the generalized morphological derivatives. Note that the PDE (24) for dilation by a set results as a special case of any of the previous three PDE's for dilations by functions g by setting $g(0) = 0$, which makes g flat. Fig. 3 shows samples of the multiscale functions δ and ε for a 1-D signal f and two different g's.

The PDE's for 1-D dilations and erosions by functions can be easily extended to the 2-D case. For example, in the 2-D case, the graph of g can be defined as the (scaled by $g(0,0)$) upper surface of 3-D structuring sets B that are, say, a unit-size cone, a sphere, or a cylinder. Then, the corresponding PDE's follow easily from the previous analysis. For example, if B is the unit sphere, then

$$g(x, y) = g(0, 0)\sqrt{1 - x^2 - y^2}, \quad x^2 + y^2 \leq 1 \tag{39}$$

and the PDE for the multiscale dilation of f by g is

$$\frac{\partial \delta}{\partial s}(x, y, s) = \sqrt{\left|\frac{\partial \delta}{\partial x}\right|^2 + \left|\frac{\partial \delta}{\partial y}\right|^2 + g^2(0, 0)}. \tag{40}$$

If B is the unit cube, then

$$g(x, y) = g(0, 0), \quad |x|, |y| \leq 1 \tag{41}$$

and the dilation PDE becomes

$$\frac{\partial \delta}{\partial s}(x, y, s) = \left|\frac{\partial \delta}{\partial x}\right| + \left|\frac{\partial \delta}{\partial y}\right| + g(0, 0). \tag{42}$$

D. Related Work

In ch. 8 of [29], Boomgaard and Smeulders have obtained similar dilation and erosion PDE's by following a different approach. They studied the propagation of the boundaries of 2-D sets (i.e., binary images) under multiscale dilation and erosion and applied these ideas to the propagation of the graph of signals under multiscale function dilation and erosion. Their work has the constraint of requiring structuring

elements with smooth boudaries, namely, they require that the structuring sets B be strictly convex and have a boundary possessing a unique normal at each point. Similarly, they require that the structuring functions g be strictly concave and have an inverse gradient function everywhere. Thus, although their work can deal with some smooth functions g of infinite support (e.g., a parabola) or of compact support whose graph does not contain linear segments, it cannot directly deal with the practically useful cases of, say in 1-D, a triangular, or rectangular, or flat function g (and correspondingly a diamond, or square, or horizontal segment for the set B). In contrast, our approach also allows for structuring elements with nonsmooth, or piecewise linear, or even discontinuous boundaries.

III. Multiscale Opening and Closing

Consider a signal $f : \mathbf{R}^d \to \mathbf{R}$ and a nonnegative concave structuring function $g : B \to \mathbf{R}$ with a compact support B. The multiscale morphological opening ψ and closing ϕ of f by g are defined as

$$\psi(x,s) \triangleq (f \circ g_s)(x) = [(f \ominus g_s) \oplus g_s](x) \tag{43}$$

$$\phi(x,s) \triangleq (f \bullet g_s)(x) = [(f \oplus g_s) \ominus g_s](x). \tag{44}$$

There is a simple geometrical interpretation [16] of the action of the opening:

$$(f \circ g)(x) = \sup_{g(x-y)+c \le f(x)} \{g(x-y) + c\}. \tag{45}$$

Thus, $f \circ g$ is the upper envelope of all shifted (in argument and amplitude) versions of g that can fit below the graph of f. There is a similar geometrical interpretation for the closing.

If g is flat, it is known [20], [24] that the compactness and convexity of B are sufficient to guarantee the following monotone structure in ψ and ϕ:

$$r < s \Longrightarrow \psi(x,r) \ge \psi(x,s) \text{ and } \phi(x,r) \le \phi(x,s) \forall\, x \tag{46}$$

and a semigroup structure for the multiscale operators $\mathcal{O}_s(f) = f \circ sB$ and $\mathcal{C}_s(f) = f \bullet sB$, where the binary operation of the semigroup is the maximum:

$$\mathcal{O}_s(\mathcal{O}_r(f)) = \mathcal{O}_{\max(r,s)}(f) \tag{47}$$

$$\mathcal{C}_s(\mathcal{C}_r(f)) = \mathcal{C}_{\max(r,s)}(f). \tag{48}$$

It can be shown that the same algebraic structure exists for openings/closings by concave and compact-support nonflat g's.

Perhaps the simplest way to generate the above multiscale openings and closings using PDE's would be to implement them serially as compositions of multiscale erosions and dilations. Specifically, $\psi(x,s)$ could be obtained by running the erosion PDE for $\varepsilon(x,r)$ over scales $r \in [0,s]$ with initial condition $\varepsilon(x,0) = f(x)$ and then running the dilation PDE for $\delta(x,r)$ over scales $r \in [0,s]$ with initial condition $\delta(x,0) = \varepsilon(x,s)$.

Alternatively, for 1-D openings by sets, the following differential-difference equation models the scale evolution of the opening. Consider a differentiable function $f : \mathbf{R} \to \mathbf{R}$, and let $g : B \to \{0\}$ be flat with $B = [-1,1]$. As s increases, the opening $\psi(x,s) = (f \circ sB)(x)$ becomes smaller because the peaks of f that have width $\le 2s$ are cut down (see Fig. 2(c) for an example of the function $\psi(x,s)$). In the process, the opening creates some flat plateaus under the peaks of f whose length increases with s, as shown in Fig. 4. Referring to Fig. 4, consider some (indexed by i) peak point $x = p_i$, where f has a local maximum, surrounded by two valley points v_i, v_{i+1}, where f has local minima. Let $r_i \in [p_i, v_{i+1}]$ and $r_i - 2s \in [v_i, p_i]$ be the right and left end points of x intervals of length $2s$ such that $\psi(r_i,s) = \psi(r_i - 2s, s) = f(r_i)$. These intervals are the supports of the flat plateaus created by the opening. Now, let $s \to s + \Delta s$ and $\psi \to \psi + \Delta\psi$. Then, as the geometry of Fig. 4 implies

$$\frac{-\Delta\psi}{\left|\frac{\partial\psi}{\partial x}(r_i - 2s, s)\right|} + \frac{-\Delta\psi}{\left|\frac{\partial\psi}{\partial x}(r_i, s)\right|} = 2\Delta s. \tag{49}$$

Hence, by letting $\partial\psi/\partial s = \lim_{\Delta s \to 0} \Delta\psi/\Delta s$, we obtain

$$\frac{\partial\psi}{\partial s}(x,s) = \frac{-2}{\left|\frac{\partial\psi}{\partial x}(r_i - 2s, s)\right|^{-1} + \left|\frac{\partial\psi}{\partial x}(r_i, s)\right|^{-1}} \quad \text{if } x \in [r_i - 2s, r_i] \tag{50}$$

and

$$\frac{\partial\psi}{\partial s}(x,s) = 0 \text{ if } x \in (v_i, r_i - 2s) \cup (r_i, v_{i+1}) \tag{51}$$

where $\partial\psi/\partial x$ are one-sided derivatives, and

$$r_i(s) = \inf\{x \ge p_i : \psi(x,s) = f(x)\}. \tag{52}$$

Similarly, by replacing, in the opening differential-difference equation, the -2 with +2 and the peak with valley points, a corresponding equation results for the multiscale closing ϕ. Since the opening differential-difference equation acts only on the signal's peaks, whereas the closing differential-difference equation acts only on the valleys, we can also combine both rules into a single differential-difference equation that models the evolution of the multiscale *opening-closing*, which is the composition of opening and closing that smooths signals similarly to a median [16].

Extending the above opening differential-difference equation to 2-D signals f and 2-D sets B presents several problems because the geometry of the 2-D flat plateaus created by the opening are not related to the geometry of the 2-D set B as simply as in the 1-D case. Note, however, that pointwise maxima of openings by 1-D line segments oriented in different directions are useful for smoothing 2-D images by preserving their line structures, as shown in Fig. 1. Hence, the derived 1-D opening differential-difference equation is also useful for 2-D filtering applications.

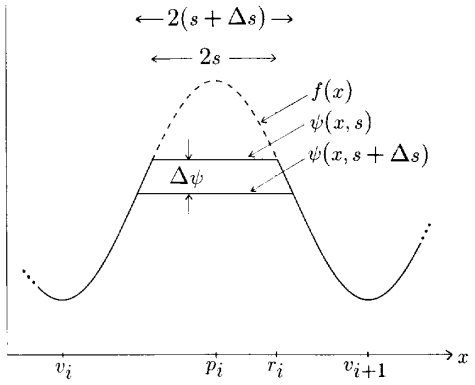

Fig. 4. Multiscale opening at scales s and $s + \Delta s$.

IV. Discussion

In conclusion, we have developed some new PDE's of the evolution type that model continuous multiscale morphological operators, of the shrink/expand or smoothing type, as dynamical systems. These PDE's suggest new ways to view and implement nonlinear multiscale filtering.

The analysis presented here suggests a rather natural way to think about and classify continuous-scale signal operators. If $\mathcal{T}_s(f)$ denotes the output of a multiscale operator at scale s applied to a signal f, then $\mathcal{T}_s$ is said to satisfy the semigroup property if $\mathcal{T}_s[\mathcal{T}_r(f)] = \mathcal{T}_{r+s}(f)$. All the multiscale erosions and dilations discussed in this paper satisfy this property when the scale s is the size of the compact convex structuring element with respect to a unit-size prototype. In addition, the linear convolution with multiscale Gaussian functions satisfies this property when the scale s is proportional to the variance of the Gaussian. Multiscale openings and closings, although they do not have an additive semigroup structure, can be expressed as compositions of operators that do satisfy this rule. Consider next the generator of the semigroup

$$\mathcal{G}[\mathcal{T}_s(f)] = \lim_{r \to 0} \frac{\mathcal{T}_{s+r}(f) - \mathcal{T}_s(f)}{r}.$$

If this limit exists in some suitable sense, it may happen that the limit is a differential operator: linear as in the case of Gaussian convolutions or nonlinear as in the case of dilations/erosions. Alternatively, it may happen that it is a combination of differential and difference operators as we have seen in the case of opening and closing. If it is a differential operator of first order, the differential equation is of hyperbolic type, and $\mathcal{T}_s(f)$ can be expected to evolve by shifting without smoothing. If it is second order and elliptic, one can expect that it will smooth f via diffusion [28].

We note that there is a large class of analog nonlinear filters that can be used as multiscale signal operators. However, unless they satisfy a semigroup property with respect to the scale, one cannot expect to find an infinitesimal generator in the way we have done in this paper. We presented PDE's for a few important multiscale nonlinear operators, i.e., erosions and dilations, and showed how to use them to generate openings and closings. However, to indicate some of the problems encountered in other types of multiscale nonlinear filters, we make a brief remark about analog rank-order and median filters [8], [14], which are closely related to morphological filters [16]. The output of a continuous-scale pth *rank-order* (or percentile) operator acting on an input 1-D real-valued differentiable function f with respect to the window $[-s, s]$ is defined at point x and scale s for $0 < p < 1$ as

$$\xi(x,s) = v \text{ iff } \text{Length}\{y : f(y) \geq v \text{ and } |y - x| \leq s\} = 2ps$$

where $\xi(x,0) = f(x)$. The *median* filter is the special case where $p = 0.5$. Fig. 5 illustrates the geometry underlying the change $\xi \mapsto \xi + \Delta\xi$ of the multiscale function due to the scale change $s \mapsto s + \Delta s$ at some point x. Referring to the notation in Fig. 5, for small changes Δs and $\Delta\xi$, we have

$$2p(s + \Delta s) = 2ps - \sum_i \Delta x_i + Q(f,x,s)\Delta s \tag{53}$$

where

$$Q(f,x,s) = H[f(x+s) - \xi(x,s)] + H[f(x-s) - \xi(x,s)]$$

and H is the unit step function defined as $H(x) = 1$ if $x \geq 0$ and $H(x) = 0$ if $x < 0$. In the limit as $\Delta s \to 0$, we also have

$$\Delta\xi = \Delta x_i \left| \frac{df}{dx}(x_i) \right| \tag{54}$$

for points x_i such that

$$\xi(x_i, s) = f(x_i), \quad x_i \in [x - s, x + s] \tag{55}$$

Combining the equations above yields in the limit

$$\frac{\partial \xi}{\partial s}(x,s) = \frac{Q(f,x,s) - 2p}{\sum_i \left| \frac{df}{dx}(x_i) \right|^{-1}}. \tag{56}$$

Note that, in contrast to multiscale erosions and dilations, the multiscale rank-order operators do not satisfy a semigroup rule. Hence, the relationship given above is not as useful as the PDE's derived for dilations and erosions. The infinitesimal generation rules for multiscale rank-order operators are signal dependent (since they depend on slopes of f at specific level-crossing points).

Finally, we have studied in this paper nonlinear PDE's of first order that can model multiscale morphological erosions, dilations, and their compositions, openings, and closings. The openings and closings are nonlinear smoothers. The classical diffusion PDE (3) is a linear second-order PDE that models the multiscale linear smoothing via Gaussian convolutions. Given that both linear and nonlinear smoothers enjoy particular advantages, it would be interesting to develop hybrid multiscale smoothing schemes that combine both characteristics. Toward this goal, evolutionary PDE's for smoothing 1-D signals $f(x)$ such as

$$\frac{\partial \psi}{\partial s} = a \left| \frac{\partial \psi}{\partial x} \right| + b \frac{\partial^2 \psi}{\partial x^2} \tag{57}$$

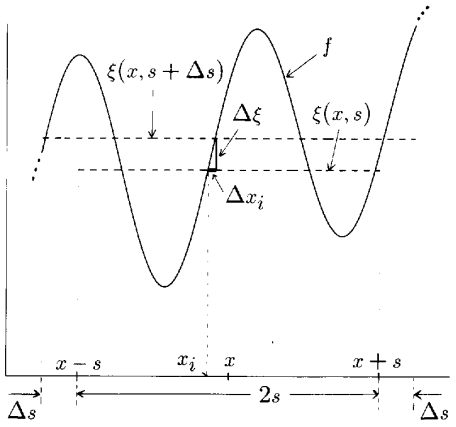

Fig. 5. Multiscale median filtering. Solid line shows the original signal f around a point x. The two horizontal dashed lines show the median values of f over two windows of scale s and $s + \Delta s$ centered at x.

$$\psi(x, 0) = f(x)$$

might be interesting, where ψ is the generated multiscale function. The coefficients a and b could be constant or varying and their relative values determine the percent of nonlinear versus linear smoothing. It remains to be seen whether or not, for specific applications of multiscale smoothing, one can identify coefficients that will lead to useful signal processing techniques.

ACKNOWLEDGMENT

The authors wish to thank C.-S. Fuh for preparing Fig. 1.

REFERENCES

[1] J. Babaud, A. Witkin, M. Baudin, and R. Duda, "Uniqueness of the Gaussian kernel for scale-space filtering," *IEEE Trans. Patt. Anal. Mach. Intell.*, vol. PAMI-8, pp. 26–33, Jan. 1986.
[2] S. Beucher and C. Lantuejoul, "Use of watersheds in contour detection," *Proc. Int. Workshop Image Processing: Real-time Edge Motion Detection/Estimation* (Rennes, France), 1979.
[3] R. W. Brockett, "Dynamical systems that sort lists, diagonalize matrices and solve linear programming problems," *Linear Algebra and its Applications*, vol. 146, pp. 79–91, 1991.
[4] R. W. Brockett and P. Maragos, "Evolution equations for continuous-scale morphology," in *Proc. IEEE Int. Conf. Acoust., Speech, Signal Processing* (San Francisco, CA), Mar. 1992.
[5] J. M. Burgers, *The Nonlinear Diffusion Equation: Asymptotic Solutions and Statistical Problems*. New York: Reidel, 1974.
[6] P. J. Burt and E. H. Adelson, "The Laplacian pyramid as a compact image code," *IEEE Trans. Commun.*, vol. COM-31, pp. 532–540, Apr. 1983.
[7] M. Chen and P. Yan, "A multiscaling approach based on morphological filtering," *IEEE Trans. Patt. Anal. Mach. Intell.*, vol. 11, pp. 694–700, July 1989.
[8] J. P. Fitch, E. J. Coyle, and N. C. Gallagher, "The analog median filter," *IEEE Trans. Circuits Syst.*, vol. CAS-33, pp. 94–102, Jan. 1986.
[9] R. M. Haralick, X. Zhuang, C. Lin, and J. S. J. Lee, "The digital morphological sampling theorem," *IEEE Trans. Acoust. Speech, Signal Processing*, vol. 37, pp. 2067–2090, Dec. 1989.
[10] R. Hummel and R. Moniot, "Reconstructions from zero crossings in scale space," *IEEE Trans. Acoust. Speech, Signal Processing*, vol. 37, pp. 2111–2130, Dec. 1989.
[11] J. J. Koenderink, "The structure of images," *Biol. Cybern.*, vol. 50, pp. 363–370, 1984.
[12] P. D. Lax, "Hyperbolic systems of conservation laws and the mathematical theory of schock waves," SIAM, Philadelphia, 1973.
[13] L. Alvarez, P.-L. Lions, and J.-M. Morel, "Image selective smoothing and edge detection by nonlinear diffusion," *SIAM J. Numer. Anal.*, vol. 29, pp. 845–866, June 1992.
[14] H. G. Longbotham and A. C. Bovik, "Comments on "The analog median filter," *IEEE Trans. Circuits and Systems*, vol. 36, p. 310, Feb. 1989.
[15] P. Maragos, "Pattern spectrum and multiscale shape representation," *IEEE Trans. Patt. Anal. Machine Intelli.*, vol. 11, pp. 701–716, July 1989.
[16] P. Maragos and R. W. Schafer, "Morphological filters—Parts I and II," *IEEE Trans. Acoust. Speech and Signal Processing*, vol. ASSP-35, pp. 1153–1184, Aug. 1987; *ibid*, vol. 37, p. 597, Apr. 1989.
[17] ——, "Morphological systems for multidimensional signal processing," *Proc. IEEE*, vol. 78, pp. 690–710, Apr. 1990.
[18] P. Maragos and F. K. Sun, "Measuring the fractal dimension of signals: morphological covers and iterative optimization," *IEEE Trans. Signal Processing*, vol. 41, pp. 108–121, Jan. 1993.
[19] D. Marr, *Vision* San Francisco: Freeman, 1982.
[20] G. Matheron, *Random Sets and Integral Geometry*. New York: Wiley, 1975.
[21] P. Perona and J. Malik, "Scale-space and edge detection using anisotropic diffusion," *IEEE Trans. Patt. Anal. Machine Intell.*, vol. 12, pp. 629–639, July 1990.
[22] A. Rosenfeld (Ed.), *Multiresolution Image Processing and Analysis*. New York: Springer Verlag, 1984.
[23] D. Schonfeld and J. Goutsias, "Optimal morphological pattern restoration from noisy binary images," *IEEE Trans. Pattern Anal. Machine Intell.*, vol. 13, pp. 14–29, Jan. 1991.
[24] J. Serra, *Image Analysis and Mathematical Morphology*. New York: Academic, 1982.
[25] J. Serra (Ed.), *Image Analysis and Mathematical Morphology, vol. 2: Theoretical Advances*. New York: Academic, 1988.
[26] J. Serra and L. Vincent, "An overview of morphological filtering," *Circuits, Systems Signal Processing*, vol. 11, no. 1, pp. 47–108, 1992.
[27] S. R. Sternberg, "Grayscale morphology," *Comput. Vision, Graphics Image Processing*, vol. 35, pp. 333–355, 1986.
[28] J. Smoller, *Shock Waves and Reaction-Diffusion Equations*. Berlin: Springer-Verlag, 1982.
[29] R. van der Boomgaard, "Mathematical morphology: Extensions towards computer vision", Ph.D. Thesis, Univ. of Amsterdam, 1992.
[30] K. C. Chou, A. S. Willsky, A. Benveniste, and M. Basseville, "Recursive and iterative estimation algorithms for multiresolution stochastic processes," in *Proc. IEEE Conf. Decision Control (CDC '89)*, 1989.
[31] A. P. Witkin, "Scale-space filtering," in *Proc. Int. Joint Conf. Artif. Intell.* (Karlsruhe), 1983.
[32] J. W. Woods and S. D. O'Neil, "Subband coding of images," *IEEE Trans. Acoust. Speech Signal Processing*, vol. ASSP-34, pp. 1278–1288, Oct. 1986.
[33] A. L. Yuille and T. Poggio, "Scaling theorems for zero crossings," *IEEE Trans. Patt. Anal. Mach. Intell.*, vol. PAMI-8, pp. 15–25, Jan. 1986.

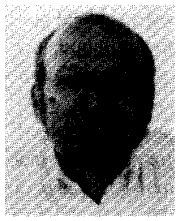

Roger W. Brockett (F'74) received the B.S., M.S. and Ph.D. degrees from Case Western Reserve University, Cleveland, OH, and joined the Department of Electrical Engineering at the Massachusetts Institute of Technology, Cambridge, in 1963 as an Assistant Professor and Ford Foundation Fellow, working in automatic control.

In 1969, he was appointed Gordon McKay Professor of Applied Mathematics in the Division of Applied Sciences at Harvard. His present position is An Wang Professor of Electrical Engineering and Computer Sciences at Harvard. Experimental and theoretical aspects of robotics, including aspects of manipulation, computer control, and sensor data fusion, are the focus of his present work. In addition to being Associate Director of the Brown-Harvard-MIT Center for Intelligent Control Systems, he also collaborates with colleagues at the University of Maryland through the Maryland-Harvard NSF Engineering Research Center on Systems Engineering.

Over the past 25 years, Dr. Brockett has been involved in the professional activities of IEEE, SIAM, and AMS, having served on the advisory committees and editorial boards for several groups in these societies. In 1989, he received the American Automatic Control Council's Richard E. Bellman Award, and in 1991, he received the IEEE Control Systems and Engineering Field Award. He is a member of the National Academy of Engineering.

Petros Maragos (S'81–M'85–SM'91) received the Diploma degree in electrical engineering from the National Technical University of Athens, Greece, in 1980 and the M.S.E.E. and Ph.D. degrees from the Georgia Institute of Technology, Atlanta, in 1982 and 1985.

In 1985, he joined the faculty of the Division of Applied Sciences at Harvard University, where he worked as Assistant (1985–1989) and Associate Professor (1989–1993) of Electrical Engineering. During the fall of 1992, he was a Visiting Professor at the National Technical University of Athens. In 1993, he joined the faculty at Georgia Institute of Technology, where he is currently an Associate Professor of Electrical and Computer Engineering. His research activities have been in the general areas of signal processing, communications, pattern recognition and their applications to image processing and computer vision, and computer speech processing and recognition.

Dr. Maragos has been involved in several professional society activities, including Associate Editor for the IEEE TRANSACTIONS ON SIGNAL PROCESSING; Editorial board member for the Journal of Visual Communication and Image Representation; General Chairman for the 1992 SPIE Conference on Visual Communications and Image Processing, Boston; Member of the IEEE DSP Technical Committee; Vice-President of the International Society for Mathematical Morphology. In 1987, he received a National Science Foundation Presidential Young Investigator Award for his work in signal and image processing. He is also the recipient of the IEEE Acoustics, Speech, and Signal Processing Society's 1988 Paper Award for his paper 'Morphological Filters' and the corecipient of the IEEE Signal Processing Society's 1994 Senior Award for his paper "Energy Separation in Signal Modulations with Application to Speech Analysis."